ELSEVIER

Signal Processing 80 (2000) 397–411

SIGNAL PROCESSING

www.elsevier.nl/locate/sigpro

Time-scale analysis of abrupt changes corrupted by multiplicative noise

Marie Chabert*, Jean-Yves Tourneret, Francis Castanie

ENSEEIHT/GAPSE, 2, rue Camichel BP7122, 31071 Toulouse, France

Received 24 April 1998; received in revised form 5 October 1999

Abstract

Multiplicative Abrupt Changes (ACs) have been considered in many applications. These applications include image processing (speckle) and random communication models (fading). Previous authors have shown that the Continuous Wavelet Transform (CWT) has good detection properties for ACs in additive noise. This work applies the CWT to AC detection in multiplicative noise. CWT translation invariance allows to define an AC signature. The problem then becomes signature detection in the time-scale domain. A second-order contrast criterion is defined as a measure of detection performance. This criterion depends upon the first- and second-order moments of the multiplicative process's CWT. An optimal wavelet (maximizing the contrast) is derived for an ideal step in white multiplicative noise. This wavelet is asymptotically optimal for smooth changes and can be approximated for small AC amplitudes by the Haar wavelet. Linear and quadratic suboptimal signature-based detectors are also studied. Closed-form threshold expressions are given as functions of the false alarm probability for three of the detectors. Detection performance is characterized using Receiver Operating Characteristic (ROC) curves computed from Monte-Carlo simulations.

Zusammenfassung

Multiplikative Abrupte Änderungen (AC) wurden in vielen Anwendungen betrachtet. Beispiele solcher Anwendungen sind die Bildverarbeitung (speckle) und Zufallsmodelle in der Übertragungstechnik (Schwund). In früheren Arbeiten wurde gezeigt, daß die kontinuierliche Wavelet-Transformation (CWT) gute Detektionseigenschaften für ACs in additivem Rauschen besitzt. In der vorliegenden Arbeit wird die CWT auf die AC-Detektion in multiplikativem Rauschen angewandt. Die Verschiebungsinvarianz der CWT erlaubt die Definition einer AC-Signatur. Das Problem besteht dann darin, eine Signatur im Zeit-Maßstabs-Bereich zu detektieren. Es wird ein Kontrastkriterium zweiter Ordnung als Maß für die Leistungsfähigkeit von Detektoren definiert. Dieses Kriterium hängt von den Momenten erster und zweiter Ordung der CWT des multiplikativen Prozesses ab. Ein optimales Wavelet, welches den Kontrast maximiert, wird für einen idealen Sprung in weißem multiplikativem Rauschen hergeleitet. Dieses Wavelet ist asymptotisch optimal für glatte Änderungen, und es kann für kleine AC-Amplituden durch das Haar-Wavelet angenähert werden. Lineare und quadratische suboptimale Detektoren, die auf Signaturen beruhen, werden ebenfalls studiert. Für drei der Detektoren werden geschlossene Ausdrücke für die Schwelle als Funktion der Fehlalarmwahrscheinlichkeit angegeben. Die Leistungsfähigkeit der Detektoren wird mittels Receiver Operating Characteristic (ROC) Kurven charakterisiert, welche mittels Monte-Carlo-Simulationen berechnet wurden.

* Corresponding author. Tel.: + 33-561-58-83-67; fax: + 33-567-58-82-37.
E-mail address: chabert@len7.enseeiht.fr (M. Chabert)

0165-1684/00/$ - see front matter
PII: S0165-1684(99)00139-5

Résumé

Cette étude concerne l'application de la Transformée en Ondelette Continue (TOC) à la détection de ruptures dans un bruit multiplicatif. L'invariance par translation de la TOC permet de définir une signature temps-échelle de la rupture. Le problème de détection est alors envisagé comme une recherche de signature dans le domaine temps-échelle. Un critère de contraste permet de classer les ondelettes selon leur capacité à séparer les deux hypothèses. Ce contraste s'exprime en fonction des moments du premier et du second ordre de la TOC du processus. Une ondelette optimale, maximisant ce contraste, est obtenue dans le cas d'un échelon multiplié par un bruit blanc. Cette ondelette peut être approchée par l'ondelette de Haar pour de faibles valeurs de l'amplitude de la rupture. Elle est asymptotiquement optimale (c'est-à-dire pour de grandes échelles) pour une rupture non abrupte (rampe, sigmoïde ...). Des détecteurs linéaires et quadratiques sous-optimaux basés sur la signature temps-échelle sont ensuite étudiés. La mise en oeuvre de ces détecteurs est simple. Une expression du seuil de détection en fonction de la probabilité de fausse alarme est donnée pour trois des détecteurs. Leurs performances, obtenues par simulations de Monte Carlo, sont présentées sous la forme de courbes Caractéristiques Opérationnelles du Récepteur (COR), pour différentes amplitudes de la rupture.

Keywords: Abrupt change; Continuous wavelet transform; Contrast; Multiplicative noise; Suboptimal detection

1. Introduction and problem formulation

Many signal and image processing applications require the detection and estimation of rapid changes in first- and second-order moments of an observed process [1]. These rapid changes (denoted Abrupt Changes (ACs)) are separated by time intervals where the moments are constant or slowly varying. Their localization is needed for segmentation purposes and object contour extraction [1]. AC detection requires specific algorithms. Indeed, adaptive algorithms are effective for tracking slow signal variations but fail when ACs occur. The Continuous Wavelet Transform (CWT) provides efficient detection of AC embedded in additive stationary noise [8,16]. Here, the original contribution is use of the CWT for AC detection in multiplicative noise.

The observed process is modelled as the product of a signal and a noise process. This model has been studied in many signal and image processing applications. Multiplicative process effectively models images produced by coherent radiation imaging systems such as Synthetic Aperture Radar (SAR) [3] or LASER [13]. These multiplicative models also describe fading phenomena in communications [29]. They model Doppler effects caused by changes in target orientation for radar and sonar applications [2]. Multiplicative models can also represent composite random processes. For example, Bernoulli–Gaussian models are useful for the joint detection-estimation of random impulses [14]. This study is restricted to multiplicative processes which are the product of a deterministic signal and a stationary random process. AC detection can be expressed as a simple binary hypothesis testing problem:

- *Under hypothesis* H_0, the observed process $y(t)$ is stationary white noise $x(t)$ with mean $m_x \neq 0$ and power spectral density N_x:

$$y(t) = x(t), \quad t \in \Omega \tag{1}$$

  where Ω is the observation interval. In practical applications, the multiplicative noise is generally non-zero mean (for instance in SAR image processing, the multiplicative noise is Gamma distributed with mean 1 and variance $1/L$ where L is the number of looks).
- *Under hypothesis* H_1, the observed process is the product of the deterministic signal $s(t)$ and the previously defined noise process $x(t)$:

$$y(t) = x(t)s(t) = x(t)\left[1 + Af\left(\frac{t - t_0}{a_0}\right)\right]$$

$$= x(t)[1 + Af_0(t)] \tag{2}$$

$$t \in \Omega,\ A \geqslant 0,\ a_0 > 0,\ t_0 > 0 \tag{3}$$

$s(t)$ is the change with parameter vector $\boldsymbol{\theta} = (A, t_0, a_0)^t$ (amplitude, instant, dilation). This signal models a transition from 1 to $1 + A$. The function f characterizes the transition shape, is assumed positive and bounded, and satisfies

$$f(t) = 0 \text{ for } t \leqslant -T \quad \text{and} \quad f(t) = 1 \text{ for } t \geqslant T \tag{4}$$

f may be a step [3], a sigmoid [19], a ramp [22, p. 399], etc. Note that when a_0 approaches zero, $s(t)$ approaches an ideal step of amplitude A at position t_0.

The Bayesian or maximum likelihood approach can be used for AC detection when the probability density functions (pdf's) of the various processes and the appropriate priors are known [27]. However, these approaches can be intractable for non-Gaussian signals with known pdf's. Wavelet-based methods are proposed here as an alternative to statistical methods.

This paper is organized as follows. Section 2 reviews the main definitions and properties of the CWT. A multiplicative AC signature can be defined because of CWT translation invariance. Then, the detection problem becomes a signature detection problem in the time-scale domain. Section 3 studies the statistical properties of the multiplicative process's CWT [4]. The first- and second-order moments are derived for the observed process's CWT under both hypotheses. A step and a polynomial singularity in white noise are studied. Section 4 deals with suboptimal detection and contrast. A second-order contrast measure is defined. This contrast measure is used to find the optimal detection wavelet. Section 4.1 shows that the complementary deflection criterion is useful for the AC detection problem in multiplicative noise. The complementary deflection measures a "signature-to-noise ratio" in the time-scale domain. Section 4.2 derives an optimal wavelet (maximizing the complementary deflection) for an ideal step embedded in white multiplicative noise. This wavelet is asymptotically optimal for smoothed changes. Section 5 studies linear and quadratic signature-based detectors. The linear test statistics consist of either the sum along scales of the CWT or the sum along scales of its correlation with an ideal signature. The quadratic test statistics have a similar structure except that the CWT is replaced by the scalogram. In both cases, the detection is achieved by thresholding. The performance of these detectors is evaluated by means of ROC curves. Closed-form expressions are also given for the thresholds as functions of the false alarm probability for three detectors.

2. Background

2.1. The continuous wavelet transform (CWT)

Time-frequency and time-scale representations have been developed because effective tools have been lacking for dealing with non-stationary signals. The Fourier transform is a useful global representation for stationary signals. However, an abrupt signal variation is spread over the entire frequency axis. The Fourier basis functions localize in frequency but not in time. The CWT decomposes a signal into a family of functions localized both in time and frequency. The family $\{\psi_{a,\tau}\}_{a\in\mathbb{R}^*,\tau\in\mathbb{R}}$ is constructed by dilation and translation of a function ψ (denoted the mother wavelet) where a is the dilation parameter and τ is the translation parameter [7,17,24,30]. The CWT of $y(t)$ (associated with this analyzing function family) is defined by

$$C_y(a,\tau) = \int_{\mathbb{R}} y(t)\psi^*_{a,\tau}(t)\,\mathrm{d}t \tag{5}$$

with

$$\psi_{a,\tau}(t) = a^{-1/2}\psi\left(\frac{t-\tau}{a}\right), \quad a\in\mathbb{R}^*,\ \tau\in\mathbb{R}. \tag{6}$$

The superscript "$*$" denotes complex conjugation. The transform admits a reconstruction formula:

$$y(t) = \frac{1}{C_\psi}\iint_{\mathbb{R}\times\mathbb{R}} C_y(a,\tau)\psi_{a,\tau}(t)\frac{\mathrm{d}a\,\mathrm{d}\tau}{a^2} \tag{7}$$

if ψ satisfies the so-called "admissibility condition" [7]:

$$C_\psi = 2\pi\int_{\mathbb{R}} |\xi|^{-1}|\hat{\psi}(\xi)|^2\,\mathrm{d}\xi < \infty \tag{8}$$

where $\hat{\psi}$ denotes the Fourier transform of ψ. A necessary condition for admissibility is [10]

$$\int_{\mathbb{R}} \psi(t)\,\mathrm{d}t = 0 \tag{9}$$

when the Fourier Transform of ψ is continuous. More restrictive regularity conditions can be required for an efficient signal analysis. Wavelets are then often designed with a specific number of vanishing moments:

$$\int_{\mathbb{R}} t^k \psi(t)\,\mathrm{d}t = 0, \quad k \in \{0,\ldots,m\}. \tag{10}$$

An important CWT property is invariance with respect to the original signal translations and dilations. The following results can be obtained [12]:

$$\mathrm{CWT}[y(t-t_0)] = C_y(a,\tau - t_0),$$

$$\mathrm{CWT}\left[\frac{1}{\sqrt{\lambda}} y\left(\frac{t}{\sqrt{\lambda}}\right)\right] = C_y\left(\frac{a}{\lambda},\frac{\tau}{\lambda}\right), \quad \forall \lambda > 0.$$

Translation invariance has been used in many detection and estimation applications (see [26,31]). Note that the CWT linearity provides a simple interpretation of the transform. No cross-terms appear, in contrast to energy distributions such as the Wigner–Ville transform.

2.2. The discretized continuous wavelet transform

Daubechies [7] defined the discretized CWT using hyperbolic sampling of the scale and translation parameters:

$$a = a_0^m, \quad \tau = n\tau_0 a_0^m, \quad a_0 > 1,\ \tau_0 > 0,\ m,n \in \mathbb{Z}. \tag{11}$$

The discretized CWT can be orthogonal or non-orthogonal, depending upon the mother wavelet ψ and the parameters a_0,τ_0. The dyadic CWT ($a_0 = 2$ and $\tau_0 = 1$) has received much attention in the literature [7,18], since it allows to build orthogonal wavelet bases. Daubechies [7] defined orthogonal dyadic bases composed of compactly supported wavelets with arbitrary regularities (including the Haar basis). Hyperbolic sampling (including dyadic sampling) is not suited to time-scale signature-based estimation and detection. Indeed, this sampling loses the translation and dilation invariance defining a signature. Moreover, hyperbolic sampling is too sparse. The scale and translation parameters must be finely sampled for joint detection estimation.

This paper computes the CWT for a very fine time-scale grid as in [12]. Translation and dilation invariances are lost because of the time and scale sampling. However, the representation remains invariant to translation of an integer number of samples. Note that the CWT samples are not orthogonal when computed on a very fine time-scale grid. This is not a problem since orthogonality is not required for AC detection. On the contrary, orthogonality imposes undesirable constraints. The constraints on the wavelet reduce to the admissibility condition when orthogonality is not required. Hence, an optimal wavelet can be chosen [31,32].

3. CWT statistical properties

For $y(t)$ a random process, the CWT defined in Eq. (5) is a random field. This section derives its first- and second-order moments under hypotheses H_0 and H_1. The study is conducted with normalized and admissible wavelets with compact support $[\Delta_1,\Delta_2]$ of length $\Delta t = \Delta_2 - \Delta_1$.

3.1. Hypothesis H_0

The observed process is stationary white noise under hypothesis H_0. The moments of $C_y(a,\tau)$ for this case were studied in [17]. Using Eq. (9), the following results can be obtained:

$$E[C_y(a,\tau)\,|\,\mathrm{H}_0] = E[C_x(a,\tau)] = m_x \int_{-\infty}^{+\infty} \psi^*_{a,\tau}(t)\,\mathrm{d}t = 0 \tag{12}$$

even when $x(t)$ is non zero-mean.

$$\mathrm{cov}[C_y(a_1,\tau_1), C_y(a_2,\tau_2)\,|\,\mathrm{H}_0] = N_x \sqrt{\frac{a_1}{a_2}} \int_{-\infty}^{+\infty} \psi^*(u)\psi\left(\frac{a_1 u + \tau_1 - \tau_2}{a_2}\right)\mathrm{d}u. \tag{13}$$

Note that if the wavelet decomposition is not orthogonal and the noise is white, the time-scale noise is correlated.

On the other hand, the orthonormal decomposition of a white stationary noise $x(t)$ gives a white sequence of stationary wavelet coefficients [16]. For a normalized wavelet, the power spectral density of $C_y(a,\tau)$ can then be expressed as:

$$S[C_y(a,\tau)\,|\,\mathrm{H}_0] = N_x \int_{\Delta_1}^{\Delta_2} |\psi(t)|^2\,\mathrm{d}t = N_x. \tag{14}$$

Consequently under hypothesis H_0, the CWT is a stationary zero-mean random process with power spectral density N_x.

3.2. *Hypothesis* H_1 – *abrupt change signature*

The observed process $y(t)$ is non-stationary under hypothesis H_1. It is the product of a deterministic signal $s(t)$ and a stationary white noise $x(t)$ with mean m_x and power spectral density N_x. Little attention has been devoted to the statistical properties of the CWT of a multiplicative process. Lu [15] expressed the correlation and power spectral density of the DWT of a zero-mean white multiplicative process in terms of the ambiguity function. Unfortunately, the results were restricted to zero-mean processes and orthogonal dyadic decompositions.

Using Eq. (9), the CWT mean value under hypothesis H_1 reads:

$$E[C_y(a,\tau)\,|\,\mathrm{H}_1] = Am_x\left[\int_{t_1}^{t_2} f_0(t)\psi^*_{a,\tau}(t)\,\mathrm{d}t + \int_{t_2}^{\tau+a\Delta_2} \psi^*_{a,\tau}(t)\,\mathrm{d}t\right] \tag{15}$$

where $t_1 = t_0 - a_0 T$ and $t_2 = t_0 + a_0 T$. The time-scale multiplicative AC signature is defined as the CWT mean value under hypothesis H_1 [8]. In what follows, AC denotes multiplicative AC. According to (15), the time-scale signature support is included in the region S defined by

$$S = \left\{(a,\tau)\in \mathbb{R}^{+*}\times\mathbb{R}^{+}\left|\frac{t_1-\tau}{a} < \Delta_2 \text{ and } \frac{t_2-\tau}{a} > \Delta_1\right.\right\}. \tag{16}$$

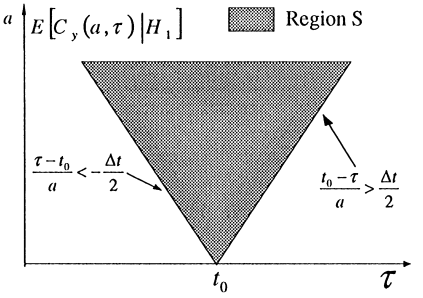

Fig. 1. Support of AC signature ($a_0 = 0$).

The CWT mean value equals zero in $R^{+*}\times R^{+} - S$. Fig. 1 shows the region S for an ideal step ($a_0 = 0$ hence $t_1 = t_2 = t_0$).

Note that the time-scale multiplicative AC signature is zero when the noise is zero-mean, contrary to the additive noise case [8]. On the other hand when the noise is non-zero mean, the AC signatures are proportional in both the additive and multiplicative cases. Consequently, the type of noise (additive or multiplicative) cannot be determined from first-order statistics [4]. The covariance of the pair $(C_y(a_1,\tau_1), C_y(a_2,\tau_2))$ can be expressed under hypothesis H_1 as:

$$\begin{aligned}\mathrm{cov}[C_y(a_1,\tau_1), C_y(a_2,\tau_2)\,|\,\mathrm{H}_1] &= \mathrm{cov}[C_y(a_1,\tau_1), C_y(a_2,\tau_2)\,|\,\mathrm{H}_0] \\ &+ AN_x\int_{-\infty}^{+\infty}[2f_0(t) + Af_0^2(t)]\,\psi^*_{a_1,\tau_1}(t)\psi_{a_2,\tau_2}(t)\,\mathrm{d}t.\end{aligned}$$

Note that when the wavelet decomposition is orthogonal, the second term differs from zero for $a_1 \neq a_2$ and $\tau_1 \neq \tau_2$. Consequently, a multiplicative white noise is transformed into a time-scale colored noise, even when the decomposition is orthogonal. The variance of $C_y(a,\tau)$ is obtained for $a_1 = a_2 = a$ and $\tau_1 = \tau_2 = \tau$:

$$\mathrm{var}[C_y(a,\tau)\,|\,\mathrm{H}_1] = N_x\left[1 + A\int_{t_1}^{\tau+a\Delta_2}[2f_0(t) + Af_0(t)^2]\,|\,\psi_{a,\tau}(t)\,|^2\,\mathrm{d}t\right]. \tag{17}$$

Eq. (17) shows the variance of $C_y(a,\tau)$ is not a constant in the time-scale domain under hypothesis H_1, contrary to the additive noise case. This property was used in [4] for distinguishing multiplicative and additive AC.

Recall that we assumed that the multiplicative noise has non-zero mean (see Eq. (1)). Consequently, the observed process $y(t)$ has a simultaneous mean and variance change. When the noise is zero mean, the observed process $y(t)$ has a variance change but no mean change. In this case, the CWT mean is zero under hypothesis H_1. However, in this case, a quadratic non-linear preprocessing allows to take advantage of CWT properties [5].

The next subsections deal with step and polynomial singularities. The effect of wavelet regularity on their time-scale signatures is studied.

3.2.1. Example 1: step singularity

Consider the fundamental example of a step-like singularity ($a_0 \to 0$) contaminated by white multiplicative noise. This model has been used for line-by-line edge detection in SAR images [3]. The multiplicative AC time-scale signature reads:

$$E[C_{y_{\text{step}}}(a,\tau)\,|\,H_1] = Am_x\sqrt{a}\int_{t_0-\tau/a}^{\Delta_2}\psi^*(t)\,dt. \tag{18}$$

The signature points to the AC instant t_0 (since $t_1 = t_2 = t_0$), whatever the wavelet regularity. For a fixed scale a, the multiplicative AC time-scale signature cross-sections are proportional to the wavelet integral (18). Consider the symmetrical Haar wavelet and the first derivative of a Gaussian (denoted FDG) defined as follows:

Symmetrical Haar wavelet

$$\psi(t) = \begin{cases} 1/\sqrt{\Delta t} & \text{if } -\Delta t/2 \leqslant t < 0, \\ -1/\sqrt{\Delta t} & \text{if } 0 \leqslant t < \Delta t/2, \\ 0 & \text{otherwise,} \end{cases} \tag{19}$$

First derivative of a Gaussian

$$\psi(t) = \sqrt{\frac{2}{\delta t \pi^{1/2}}}\frac{t}{\delta t}\exp\left[-\frac{1}{2}\left(\frac{t}{\delta t}\right)^2\right], \quad t\in\mathbb{R},\ \delta t\in\mathbb{R}^{+}*. \tag{20}$$

The multiplicative AC time-scale signature cross-sections are triangles and Gaussian functions.

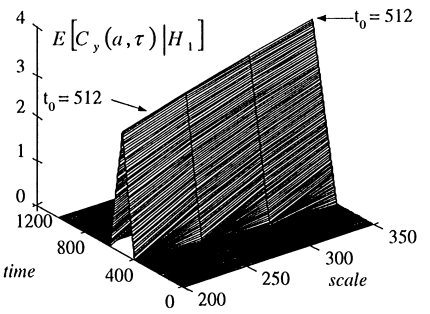

Fig. 2. Step signature ($A = 0.4, t_0 = 512$) with symmetrical Haar wavelet.

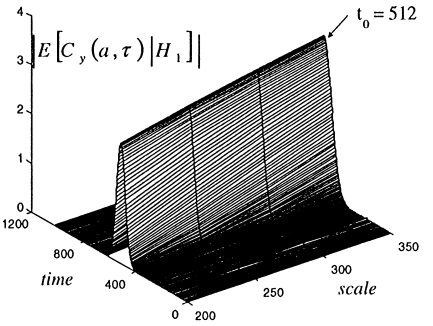

Fig. 3. Step signature ($A = 0.4, t_0 = 512$) with FDG wavelet.

These signatures are shown (Figs. 2 and 3) for parameters $t_0 = 512$ (AC instant), $A = 0.4$ (AC amplitude), $N = 1024$ (number of samples), $m_x = 1$ (multiplicative noise mean) and $N_x = 1$ (power spectral density). The signatures are conic with a maximum for $\tau = t_0$ with Haar and FDG wavelets.

The time-scale variance for a step singularity can be expressed as:

$$\text{var}[C_{y_{\text{step}}}(a,\tau)\,|\,H_1] = \begin{cases} N_x[1 + (2A + A^2)\int_{t_0-\tau/a}^{\Delta_2}|\psi(t)|^2\,dt] \\ \quad \text{for } \Delta_1 < \frac{t_0-\tau}{a} < \Delta_2, \\ N_x(1+A)^2 \quad \text{for } \frac{t_0-\tau}{a} < \Delta_1, \\ N_x \quad \text{for } \frac{t_0-\tau}{a} > \Delta_2. \end{cases} \tag{21}$$

Eq. (21) shows a constant variance for $C_y(a,\tau)$ in the two time-scale regions bordering the conic

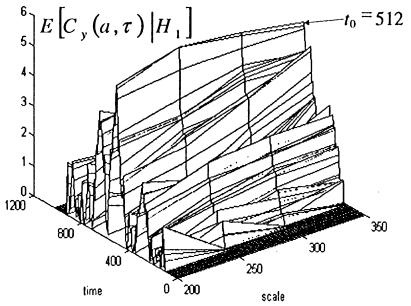

Fig. 4. CWT of a step ($A = 0.4, t_0 = 512$) embedded in multiplicative noise with Haar wavelet.

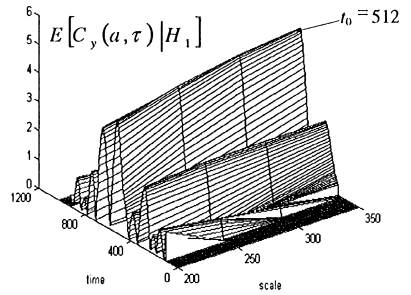

Fig. 5. CWT of a step ($A = 0.4, t_0 = 512$) embedded in multiplicative noise with FDG wavelet.

signature. The noisy multiplicative AC CWTs for the Haar and FDG wavelets are shown in Figs. 4 and 5. Clearly, a cone emerges from the noise for the Haar and FDG wavelets. The cone points to the AC instant t_0. Provided an appropriate wavelet is selected (discussed in Section 4.2), the CWT is a suitable tool for multiplicative AC estimation and detection.

Smoother transitions must be considered in many interesting cases. According to the Stone–Weierstrass theorem, any continuous function defined on a closed interval can be approached by a polynomial function [22, p. 399]. The next subsection studies polynomial singularities.

3.2.2. Example 2: polynomial singularity

A polynomial singularity is defined by

$$f(t) = \sum_{i=0}^{N} b_i t^i \quad \text{for } -T < t < T.$$

The time-scale signature in a region S can be expressed as (15):

$$E[C_y(a,\tau)\,|\,\mathrm{H}_1] = \sqrt{a}Am_x\left[\int_{(t_1-\tau)/a}^{(t_2-\tau)/a}\sum_{i=0}^{N} b_i\left(\frac{au+\tau-t_0}{a_0}\right)^i \psi^*(u)\,\mathrm{d}u + \int_{(t_2-\tau)/a}^{\Delta_2}\psi^*(u)\,\mathrm{d}u\right]. \tag{22}$$

The CWT mean depends upon the polynomial degree and the wavelet number of vanishing moments. The signature in region $s \subset S$ (defined presently) reduces to

$$E[C_y(a,\tau)\,|\,\mathrm{H}_1]_s = \sqrt{a}Am_x\int_{\Delta_1}^{\Delta_2}\sum_{i=0}^{N} b_i\left(\frac{au+\tau-t_0}{a_0}\right)^i \psi^*(u)\,\mathrm{d}u \tag{23}$$

with

$$s = \left\{(a,\tau)\in\mathbb{R}^{+*}\times\mathbb{R}^{+}\left|\frac{t_1-\tau}{a} < \Delta_1 \text{ and } \frac{t_2-\tau}{a} > \Delta_2\right.\right\}. \tag{24}$$

Consequently, if m denotes the number of vanishing moments of the wavelet and $m \geqslant N$ then $E[C_y(a,\tau)]_s = 0$. For a ramp singularity defined by

$$f(t) = \begin{cases} \frac{t+T}{2T} & t\in[-T,T], \\ 0 & t < -T, \\ 1 & t > T, \end{cases}$$

Eq. (23) reduces to

$$E[C_y(a,\tau)\,|\,\mathrm{H}_1]_s = \begin{cases} \frac{a^{3/2}Am_x}{a_0}\int_{\Delta_1}^{\Delta_2} u\psi^*(u)\,\mathrm{d}u & \text{if } m = 0, \\ 0 & \text{if } m \geqslant 1. \end{cases} \tag{25}$$

If $m \geqslant 1$, two cones are pointing one to the beginning of the polynomial singularity and the other to the end (Fig. 6). The time-scale multiplicative AC signature and the multiplicative AC CWT with Haar and FDG wavelet ($m = 0$) are shown in Figs. 7–10 for $a_0 = 200$, $t_0 = 512$ and $A = 0.4$.

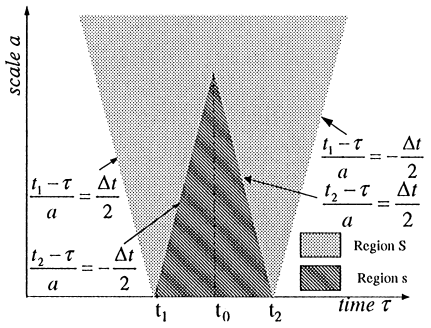

Fig. 6. Support of smoothed change signature ($a_0 \neq 0$).

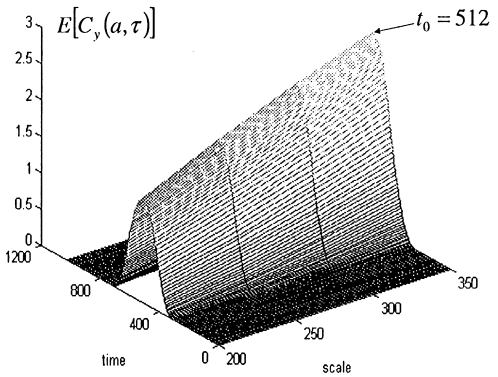

Fig. 7. Ramp signature ($A = 0.4, t_0 = 512, a_0 = 200$) with symmetrical Haar wavelet.

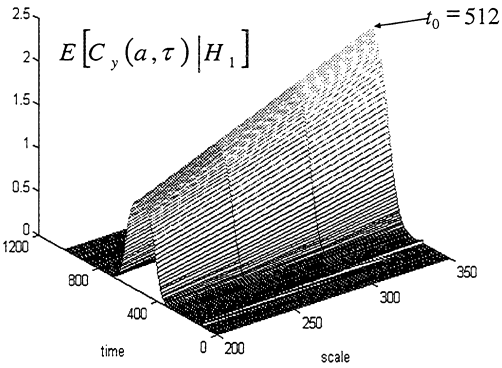

Fig. 8. Ramp signature ($A = 0.4, t_0 = 512, a_0 = 200$) with FDG wavelet.

4. Contrast in the time-scale domain

The optimal Neyman–Pearson detector has been used successfully in many signal and image applications. The Neyman–Pearson detector is optimal in the sense that it maximizes the Probability of Detection (PD) for a fixed Probability of False Alarm (PFA). The Neyman–Pearson detector determines the likelihood ratio which is a sufficient statistic for simple binary hypothesis tests [21]. The likelihood ratio is compared to a threshold which depends upon PFA. Optimal detection requires knowledge of the observed process distribution. Unfortunately, this distribution is often only partially known or too complex to derive. This problem suggests the use of suboptimal detectors. The decision, concerning the observation $y(t)$, is made using the pseudo-observation $C_y(a,\tau)$. The previous section has shown that the wavelet choice can be critical for AC detection in multiplicative noise. The best detection

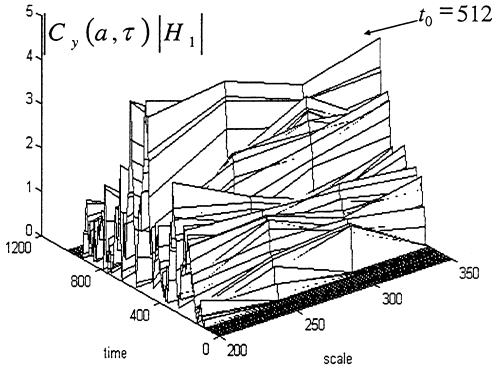

Fig. 9. CWT of a ramp ($A = 0.4, t_0 = 512, a_0 = 200$) embedded in multiplicative noise with Haar wavelet.

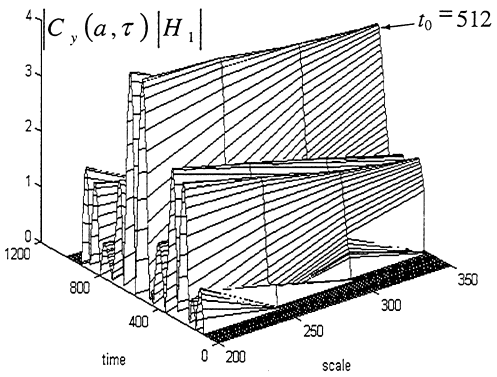

Fig. 10. CWT of a ramp ($A = 0.4, t_0 = 512, a_0 = 200$) embedded in multiplicative noise with FDG wavelet.

wavelet is defined by the selected contrast criterion.

This section is restricted to non-zero mean multiplicative noise. The contrast criterion is based upon the observed CWT mean and variance under hypotheses H_0 and H_1 (see Eqs. (12), (15), (14) and (17)). However, a similar contrast could be defined for zero-mean noise using a non-linear transformation of the observed signal [5].

4.1. Contrast criterion

The contrast criterion measures how a transform separates two hypotheses. The most popular family of contrasts is based upon second-order quality measures. A second order quality measure is defined only in terms of second-order probabilistic parameters, viz., means and covariances. A second-order contrast is related to generalized SNR when the hypotheses are "noise" and "signal and noise". The contrast for the pseudo-observation $C_y(a,\tau)$ is defined at each point of the time-scale plane (a,τ) as (cf. [11,21]):

$$\gamma_\alpha[C_y(a,\tau)] = \frac{[E[C_y(a,\tau)\,|\,H_1] - E[C_y(a,\tau)\,|\,H_0]]^2}{\mathrm{Var}_\alpha[C_y(a,\tau)]} = \frac{E[C_y(a,\tau)\,|\,H_1]^2}{\mathrm{Var}_\alpha[C_y(a,\tau)]}. \quad (26)$$

In (26), $\mathrm{Var}_\alpha[C_y(a,\tau)]$ is the variance corresponding to the mixing distribution:

$$p_\alpha(x) = (1-\alpha)p_0(x) + \alpha p_1(x) \quad \text{with } \alpha \in [0,1]$$

where $p_0(.)$ and $p_1(.)$ are the distributions of $C_y(a,\tau)$ under hypotheses H_0 and H_1. For $\alpha = 0$ and $\alpha = 1$, the criteria are usually called deflection and complementary deflection respectively [11]. The deflection and complementary deflection are used interchangeably for additive noise since the variance is the same under both hypotheses. Here, for the multiplicative AC detection problem, the complementary deflection has been chosen. It corresponds to the most restrictive contrast between the two extremes $\alpha = 0$ and $\alpha = 1$ ($\mathrm{Var}[C_y(a,\tau)\,|\,H_1] \geqslant \mathrm{Var}[C_y(a,\tau)\,|\,H_0]$ according to (14) and (17)).

The complementary deflection, denoted $\beta_f(a,\tau)$ in what follows, can be interpreted as a signature-to-noise ratio in the time-scale domain. A straightforward computation yields

$$\beta_f(a,\tau) = \frac{A^2 m_x^2}{N_x} \times \frac{\left|\int_{t_0-a_0^{\Delta_2}T}^{\tau+a\Delta_2} f_0(t)\psi^*_{a,\tau}(t)\,\mathrm{d}t\right|^2}{1 + A\int_{t_0-a_0^{\Delta_2}T}^{\tau+a\Delta_2}[2f_0(t) + Af_0(t)^2]\,|\psi_{a,\tau}(t)|^2\,\mathrm{d}t}. \quad (27)$$

4.2. Optimal wavelet

4.2.1. Definition

This section derives an optimal wavelet for the multiplicative AC detection problem. A wavelet $\psi(t)$ is optimal if it maximizes the complementary deflection denoted $\beta_f(a,\tau)$ under the constraints of normalization (28) and of the sufficient condition for admissibility (29):

$$\int_{\Delta_1}^{\Delta_2} |\psi(t)|^2\,\mathrm{d}t = 1, \quad (28)$$

$$\int_{\Delta_1}^{\Delta_2} \psi(t)\,\mathrm{d}t = 0. \quad (29)$$

Recall that (29) is required to obtain a signature under H_1 against no signature under H_0. Maximizing $\beta_f(a,\tau)$ under the constraints (28) and (29) for any AC (defined by $f_0(t)$) is a difficult problem. The next subsection studies the case of a step singularity.

4.2.2. Step singularity in white noise

For a step singularity in white noise, the complementary deflection reduces to:

$$\beta_{\mathrm{step}}(a,\tau) = a\frac{A^2 m_x^2}{N_x}\frac{P_{\psi,\xi}}{1 + vN_{\psi,\xi}}$$

$$\text{with} \quad \begin{cases} N_{\psi,\xi} = \int_\xi^{\Delta_2} |\psi(t)|^2 \mathrm{d}t, \\ P_{\psi,\xi} = |\int_\xi^{\Delta_2} \psi(t)\,\mathrm{d}t|^2, \\ v = A^2 + 2A, \\ \xi = \frac{t_0-\tau}{a}. \end{cases}$$

The contrast is proportional to the scale on the time-scale plane line D_ξ defined by $(t_0 - \tau)/a = \xi$ and consequently increases at high scales. The

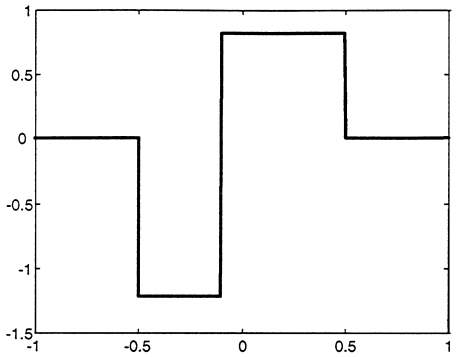

Fig. 11. Optimal wavelet for an AC embedded in white multiplicative noise ($A = 0.5$).

maximum complementary deflection is obtained for [6]:

$$\xi_{\text{opt}} = \Delta_1 + \frac{\Delta_2 - \Delta_1}{A+2}, \tag{30}$$

$$\psi_{\text{opt}}(t) = \begin{cases} C_1 = -\varepsilon\sqrt{\frac{(A+1)}{\Delta t}} & \text{for } t \in [\Delta_1, \xi_{\text{opt}}], \\ C_2 = \frac{\varepsilon}{\sqrt{(A+1)\Delta t}} & \text{for } t \in [\xi_{\text{opt}}, \Delta_2]. \end{cases} \tag{31}$$

Fig. 11 shows the optimal wavelet for an AC amplitude $A = 0.5$. Note that the optimal wavelet depends upon the AC amplitude. This may be a problem in practical applications since the AC amplitude is unknown. However, for small values of $A (A \ll 1)$, Eqs. (30) and (31) yield

$$\xi_{\text{opt}} \cong \frac{\Delta_1 + \Delta_2}{2}, \tag{32}$$

$$\psi_{\text{opt}}(t) \cong \begin{cases} C_1 = -\frac{\varepsilon}{\sqrt{\Delta t}} & \text{for } t \in [\Delta_1, \xi_{\text{opt}}], \\ C_2 = \frac{\varepsilon}{\sqrt{\Delta t}} & \text{for } t \in [\xi_{\text{opt}}, \Delta_2]. \end{cases} \tag{33}$$

This shows that the optimal wavelet can be approximated by the symmetrical Haar wavelet.

4.2.3. Smoothed change

Consider the general case of a smoothed change. The complementary deflection on the line D_ξ defined by $(t_0 - \tau)/a = \xi \in [\Delta_1, \Delta_2]$, reads:

$$\beta_f(a,\tau) = \frac{aA^2 m_x^2}{\sigma_x^2} \frac{[I_1 + I_2]^2}{1 + I_4 + (A^2 + 2A) I_3}$$

with

$$I_1 = \int_{(t_1/a)+\xi}^{(t_2/a)+\xi} f\left(\frac{at}{a_0}\right)\psi(t)\,\mathrm{d}t,$$

$$I_2 = \int_{(a_0/a)T+\xi}^{\Delta_2} \psi(t)\,\mathrm{d}t,$$

$$I_3 = \int_{(t_2/a)+\xi}^{\Delta_2} \psi^2(t)\,\mathrm{d}t,$$

$$I_4 = \int_{(t_1/a)+\xi}^{(t_2/a)+\xi} \left[\left(1 + Af\left(\frac{at}{a_0}\right)\right)^2 - 1\right]\psi^2(t)\,\mathrm{d}t,$$

$$I_5 = \int_{(-a_0/a)T+\xi}^{(a_0/a)T+\xi} \left[\left(1 + Af\left(\frac{at}{a_0}\right)\right)^4 - 1\right]\psi^2(t)\,\mathrm{d}t.$$

When the scale a goes to infinity, the integrals I_i reduce as follows:

$$\lim_{a\to+\infty} I_1 = \lim_{a\to+\infty} I_2 = \lim_{a\to+\infty} I_3 = 0,$$

$$\lim_{a\to+\infty} I_4 = \int_{\xi}^{\Delta_2} \psi(t)\,\mathrm{d}t$$

and

$$\lim_{a\to+\infty} I_5 = \int_{\xi}^{\Delta_2} \psi^2(t)\,\mathrm{d}t$$

(since the wavelet ψ and the function f are bounded). Finally

$$\beta_f(a,\tau) \sim \beta_{\text{step}}(a,\tau) \quad \text{when } a \to +\infty.$$

Consequently, the optimal wavelet for an ideal AC is asymptotically optimal (asymptotically means when $a \to +\infty$) for a smoothed change. This result shows that the CWT is asymptotically robust to the transition shape.

5. Suboptimal time-scale detectors

The CWT can be interpreted as a correlation between the observed process and a shifted scaled mother wavelet. The CWT can then be compared to a two-dimensional threshold for AC detection [9]. However, the threshold setting requires knowledge of the CWT distribution under H_0. This distribution may be unknown or difficult to derive for non-Gaussian inputs. This paper proposes four

one-dimensional CWT detectors. They correspond to a summation over scales of the CWT with possible post-processing. The summation is over several octaves in scale in order to sum decorrelated coefficients. The main purpose of summation is to obtain Gaussian statistics whatever the multiplicative noise distribution. The detectors are defined as follows:

- Detectors Γ_1 and Γ_2 correspond to a linear post-processing of the CWT. These detectors were first studied in [8] for the detection of ACs in additive stationary noise. Γ_1 computes the sum along scales of the CWT. Γ_2 computes the sum along scales of the CWT correlation with an ideal signature.
- Detectors Γ_3 and Γ_4 introduce a quadratic post-processing of the CWT and a scale dependent weighting.

5.1. *Linear post-processing* (*detectors* Γ_1 *and* Γ_2)

- *Sum along scales of the CWT*: The sum of fixed scale CWT slices reduces noise effects since the noise maxima do not propagate from one scale to another [16]. Detector Γ_1 is defined by

$$\Gamma_1(\tau) = \sum_{i=1}^{n} C_y(a_i,\tau). \tag{34}$$

  This detector does not require a priori information about the AC to be detected.
- *Time-scale correlator*: The time-scale correlator computes the sum across scales of the correlation between the observed process's CWT and an ideal 2D signature $C_{\text{ideal}}(a,\tau)$ (constructed using a priori information on the expected AC):

$$\Gamma_2(\tau) = \sum_{i=1}^{n} \int_{\mathbb{R}} C_y(a_i,t) C_{\text{ideal}}(a_i, t-\tau)\,\mathrm{d}t. \tag{35}$$

This correlation yields a smoother statistic than the previous detector. The correlation would be equivalent to time-scale matched-filtering if (i) the noise were additive, white and stationary, and (ii) the expected signal were perfectly known [9]. Here, the notion of matched filter is not defined because the noise is colored, non-stationary and non-additive in the time-scale domain [27].

The test statistics Γ_1 and Γ_2 are linear and equivalent to filtering in the time domain. The CWT allows to build this filter in the multiplicative noise case. However, the optimal Neyman Pearson detector is non-linear for this detection problem [28]. Consequently, it seems natural to study suboptimal non-linear detectors. Non-linear post-processings were already proposed for the detection and estimation in the time-scale domain. Mallat suggested to extract CWT modulus maxima for edge characterization in additive noise [17]. Multiscale products were also studied for multistep detection and estimation in additive or multiplicative noise [25]. Finally, the scalogram (squared CWT modulus) was used to build time-scale energetic detectors [10]. This paper proposes to study two quadratic detectors (denoted $\Gamma_3(\tau)$ and $\Gamma_4(\tau)$) based on the scalogram.

5.2. *Quadratic post-processing* (*detectors* Γ_3 *and* Γ_4)

- *Weighted sum of the scalogram*: $\Gamma_3(\tau)$ is a weighted quadratic formulation of $\Gamma_1(\tau)$. Going back to continuous variable, summing across scales means integrating the CWT with the measure $\mathrm{d}a$. However, the energy in the whole time-scale domain expresses as $\iint |C_y(a,\tau)|^2 \frac{\mathrm{d}a\,\mathrm{d}\tau}{a^2}$ [10]. Hence, $\mathrm{d}a/a^2$ appears as a more meaningful measure for one-dimensional energetic detectors. This suggests to define the following detector:

$$\Gamma_3(\tau) = \sum_{i=1}^{n} \frac{|C_y(a_i,\tau)|^2}{a^2}$$

- *Weighted sum of the scalogram correlation*: $\Gamma_4(\tau)$ computes the sum along scales of the scalogram correlation with an ideal scalogram

$$\Gamma_4(\tau) = \sum_{i=1}^{n} \frac{\int_{\mathbb{R}} |C_y(a_i,t)|^2 |C_{\text{ideal}}(a_i,t-\tau)|^2 \mathrm{d}t}{a^2}.$$

Note that the four test statistics $\Gamma_i(\tau)$, $i = 1,\ldots,4$, are maximum for $\tau = t_0$. This property can be used to derive AC instant estimates. These estimates do not require information about the process

distribution as is required for maximum likelihood estimation.

5.3. Detection performance

AC detection can be achieved as follows:

$$\mathrm{H}_0 \text{ is rejected if } \exists \tau \in \Omega \text{ such that } \Gamma_i(\tau) > S_i(\mathrm{PFA}) \tag{36}$$

$$\text{where PFA} = P[\text{reject } \mathrm{H}_0 \,|\, \mathrm{H}_0 \text{ true}] = \int_{S_i}^{\infty} f_0(t)\,\mathrm{d}t. \tag{37}$$

f_0 denotes the test statistic distribution under H_0. The detection performance can then be studied using Receiver Operating Characteristics (ROC) curves [29]. These curves show PD as a function of PFA. The PD (respectively PFA) computation requires knowledge of the test statistic pdf under H_1 (respectively H_0). However, when pdf's are unknown or partially known, ROC curves can be obtained numerically by comparing runs of the test statistic under H_0 and H_1 to suitable threshold values. Figs. 12 and 13 show numerical ROC curves obtained with 100 runs. The observed process is a step embedded in multiplicative white noise. The noise and AC parameters are $t_0 = 512$, $A \in \{0.1, 0.2, 0.3, 0.4, 0.5\}$, $m_x = 1$, $N_x = 1$ and $N = 1024$. The CWT is computed with the symmetrical Haar wavelet, with normalized support, for integer scales varying from $a = 1$ to 1024. Very good detection performance is obtained for an AC with amplitude $A \geqslant 0.4$ in multiplicative noise with mean $m_x = 1$ and power spectral density $N_x = 1$.

The theoretical results (optimal wavelet, contrast comparison, etc.) were obtained for white noise in this paper. The effects of noise correlation are studied through simulations. Figs. 14 and 15 show ROC curves for multiplicative colored noise modelled as a zero-mean Auto-Regressive AR process plus constant $m_x = 1$. The AR parameters are $a = [1, 0.2, 0.15]^{\mathrm{T}}$ and the driving noise spectral density is such that $N_x = 1$. The AC and CWT parameters are the same as previously. Figs. 14 and 15 show that the detection performance is not affected by noise coloration, in contrast to optimal detector performance [28]. This result emphasizes the advantage of time-scale detectors.

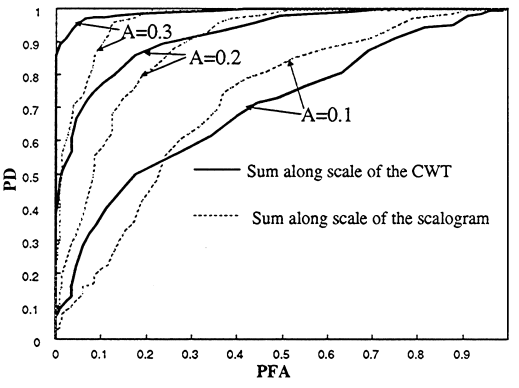

Fig. 12. ROC curves for detectors $\Gamma_1(\tau)$ and $\Gamma_3(\tau)$ (white multiplicative noise).

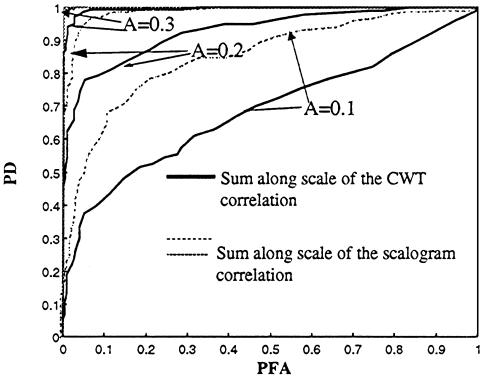

Fig. 13. ROC curves for detectors $\Gamma_2(\tau)$ and $\Gamma_4(\tau)$ (white multiplicative noise).

5.4. Comparison between linear and quadratic detectors

Figs. 12–15 allow to compare linear and quadratic detector performance for fixed noise parameters and different AC amplitudes. These figures show that Γ_4 performs better than Γ_2 but that Γ_3 performs worse than Γ_1 for low PFAs. Similar results are obtained for white and colored noise. Consequently, a quadratic post-processing does not necessarily improve performance. This improvement depends on the detector structure but also on the noise and signal parameters.

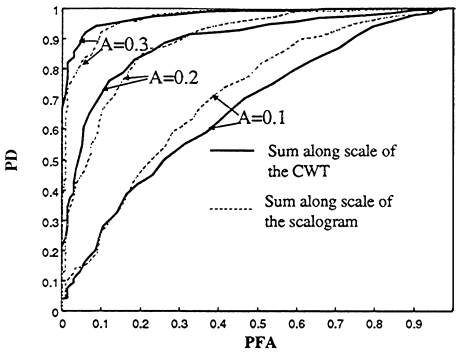

Fig. 14. ROC curves for detectors $\Gamma_1(\tau)$ and $\Gamma_3(\tau)$ (colored multiplicative noise).

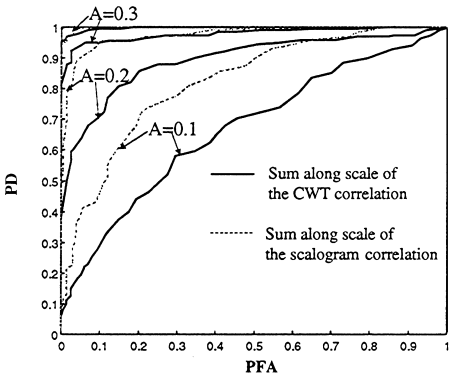

Fig. 15. ROC curves for detectors $\Gamma_2(\tau)$ and $\Gamma_4(\tau)$ (colored multiplicative noise).

Recall that the main motivation for summing across scales was to obtain approximately Gaussian test statistics for any noise distribution and any fixed τ. When the Gaussian approximation is valid, the threshold can be determined using the approximate Gaussian pdf for the test statistic under H_0 by

$$\mathrm{PFA} = \int_{\frac{S_i(pfa)-m_0^i}{\sigma_0^i}}^{\infty} \frac{1}{\sqrt{2\pi}} e^{-y^2/2}\, dy \tag{38}$$

where m_0^i and σ_0^i are the mean and standard deviation of the test statistic under H_0. Finally

$$S_i(pfa) = m_0^i + \sigma_0^i(1 - \mathrm{erf}^{-1}(\mathrm{PFA}))$$

where $\mathrm{erf}(x) = (2/\sqrt{\pi})\int_0^x e^{-t^2/2}\, dt$. Note that the threshold determination requires the knowledge of m_0^i and σ_0^i (functions of the noise mean and power spectral density). These parameters have to be estimated using noise samples in practical applications.

The use of central limit theorems (such as Liapounov or Lindeberg [23]) is not straightforward to prove the asymptotic normality of Γ_i, $i = 1,2,\ldots,4$. However, Figs. 16–19 show a comparison between the four test statistics histograms and the fitted Gaussian pdf's under hypothesis H_0 with 95% confidence intervals (computed as in [20, p. 251]). The multiplicative noise is uniformly

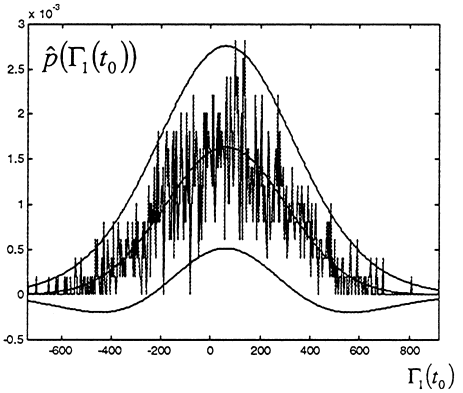

Fig. 16. Histogram of $\Gamma_1(t_0)$ and fitted Gaussian pdf with 95% confidence intervals.

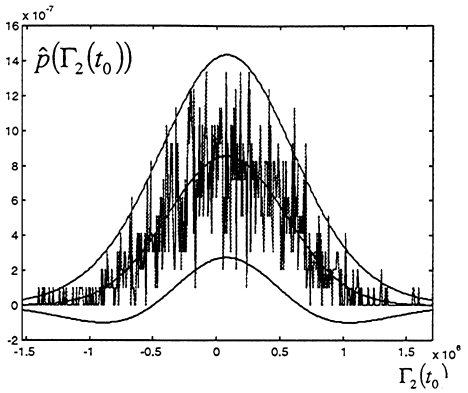

Fig. 17. Histogram of $\Gamma_2(t_0)$ and fitted Gaussian pdf with 95% confidence intervals.

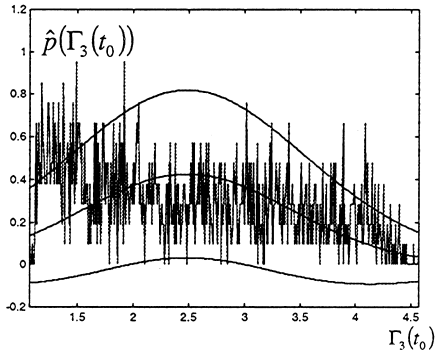

Fig. 18. Histogram of $\Gamma_3(t_0)$ and fitted Gaussian pdf with 95% confidence intervals.

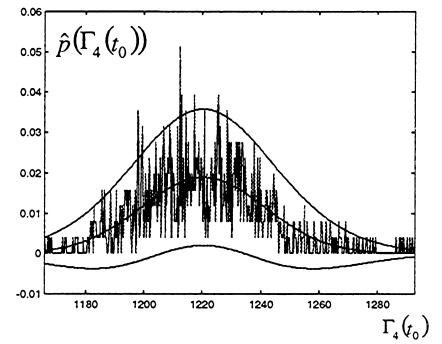

Fig. 19. Histogram of $\Gamma_4(t_0)$ and fitted Gaussian pdf with 95% confidence intervals.

distributed with $m_x = 1$ and $N_x = 1$. These figures clearly show that the Gaussian pdf is a good approximation for the pdf of $\Gamma_1(\tau)$, $\Gamma_2(\tau)$ and $\Gamma_4(\tau)$ under H_0, but not for $\Gamma_3(\tau)$. Consequently, the Gaussian approximation for $\Gamma_1(\tau)$, $\Gamma_2(\tau)$ and $\Gamma_4(\tau)$ can be used to compute the test thresholds without a priori information on the noise distribution. However, this Gaussian approximation cannot be used for detector $\Gamma_3(\tau)$.

Consequently, the use of quadratic post-processings can lead to non-Gaussian test statistics. In these cases, the threshold cannot be obtained in closed form. For this reason, quadratic post-processings should not be systematically introduced. This paper recommends the use of linear post-processings which provide approximately Gaussian test statistics and good performance for white and colored noise.

6. Conclusions

The continuous wavelet transform showed good properties for detecting abrupt changes in multiplicative noise. First and second order moments were derived for the continuous wavelet transform of the observed process. These moments defined an abrupt change signature in the time-scale domain. The complementary deflection was chosen as a contrast criterion in the time-scale domain. An optimal wavelet maximizing the complementary deflection was derived for the detection of an ideal step in white multiplicative noise. This wavelet depended upon the abrupt change amplitude and was asymptotically optimal for smooth changes. Linear and quadratic time-scale AC detectors were then compared. Threshold determination cannot always be achieved for non-linear detectors. Consequently, linear time-scale detectors have to be prefered to quadratic time-scale detectors for the detection of AC in white or colored multiplicative noise.

Acknowledgements

Thanks to Professor Neil Bershad for improving the readability of the paper. Thanks to the reviewers for their helpful comments and suggestions.

References

[1] M. Basseville, I.V. Nikiforov, Detection of Abrupt Changes: Theory and Application, Prentice-Hall, Englewood Cliffs, NJ, 1993.
[2] O. Besson, F. Castanié, On estimating the frequency of a sinusoid in autoregressive multiplicative noise, Signal Processing 30 (January 1993) 65–83.
[3] A.C. Bovik, On detecting edges in speckle imagery, IEEE Trans. Acoust. Speech Signal Process. 36 (10) (October 1988) 1618–1627.
[4] M. Chabert, J.-Y. Tourneret, F. Castanié, Additive and multiplicative jump detection using continuous wavelet transform, Proceedings of the ICASSP'96, Atlanta, 1996, pp. 3002–3005.
[5] M. Chabert, J.-Y. Tourneret, F. Castanié, Time-scale analysis of deterministic signals corrupted by zero-mean Multiplicative Noise, Proceedings of the 1997 Workshop on Nonlinear Signal and Image Processing, Michigan.
[6] M. Chabert, Détection et estimation de ruptures noyées dans un bruit multiplicatif – approches classiques et

temps-échelle, Thèse de Doctorat de l'Institut National Polytechnique de Toulouse, No. 1395, Décembre 1997.
[7] I. Daubechies, Ten Lectures on Wavelets, CBMS-NSF Regional Conference Series In Applied Mathematics, 1992.
[8] A. Denjean, F. Castanié, Mean value jump detection: a survey of conventional and wavelet based methods, in: C.K. Chui, L. Montefuso, L. Puccio (Eds.), Wavelet Theory, Algorithms and Applications, Academic Press, New York, 1994, pp. 573–584.
[9] P. Flandrin, Some aspects of nonstationary signal processing with emphasis on time-frequency and time-scale methods, in: J.M. Combes, A. Grossmann, Ph. Tchamitchian (Eds.), Wavelets: Time-Frequency Methods and Phase Space, 2nd Edition, Springer, New York, 1989, pp. 68–98.
[10] P. Flandrin, Temps-Fréquence, Traité des Nouvelles Technologies, Série Traitement du Signal, Hermès, 1993.
[11] W.A. Gardner, A unifying view of second-order measures of quality for signal classification, IEEE Trans. Comm. com-28 (1980) 807–816.
[12] A. Grossmann, R. Kronland-Martinet, J. Morlet, in: J.M. Combes, A. Grossmann, Ph. Tchamitchian (Eds.), Reading and Understanding Continuous Wavelet Transforms, Wavelets Time-Frequency Methods and Phase Space, 2nd Edition, Springer, Berlin, 1990, pp. 2–20.
[13] P.A. Kelly, H. Derin, K.D. Hartt, Adaptive segmentation of speckled images using a hierarchical random field model, IEEE Trans. Acoust. Speech Signal Process. 36 (10) (October 1988) 1628–1641.
[14] J.J. Kormilo, J.M. Mendel, Maximum likelihood detection and estimation of Bernoulli-Gaussian processes, IEEE Trans. Inform. Theory IT-28 (3) (May 1982) 482–488.
[15] C.Y. Lu, Second-order statistics of the wavelet transform of multiplicative white stochastic process, Proceedings of the ICASSP'94, 1994, pp. III21–III24.
[16] S. Mallat, S. Zhong, Characterization of signals from multiscale edges, IEEE Trans. Pattern Anal. Mach. Intell. 8 (1986) 679–698.
[17] S. Mallat, W.L. Hwang, Singularity detection and processing with wavelets, IEEE Trans. Inform. Theory 38 (2) (1992) 617–643.
[18] Y. Meyer, Orthonormal wavelets, in: J.M. Combes, A. Grossmann, Ph. Tchamitchian (Eds.), Wavelets Time-Frequency Methods and Phase Space, 2nd Edition, Springer, Berlin, 1990, pp. 21–37.
[19] A. Moghaddamjoo, M. Doroodchi, Cramer-Rao lower bound on locations of sudden changes in a steplike signal, IEEE Trans. Signal Process. 44 (10) (October 1996) 2551–2556.
[20] A. Papoulis, Probability, Random Variables and Stochastic Processes, 3rd Edition, McGraw-Hill, New York, 1991.
[21] B. Picinbono, P. Duvaut, Detection and contrast, in: C.R. Baker et al. (Eds.), Stochastic Processes in Underwater Acoustics, Lecture Notes in Control and Information Sciences, Vol. 85, 1986, pp. 181–203.
[22] B. Porat, Digital Processing of Random Signals Theory and Methods, Prentice-Hall Information and System Sciences Series, Prentice-Hall, Englewood Cliffs, NJ, 1994.
[23] A. Rényi, Calcul des Probabilités, Dunod, Paris, 1966.
[24] O. Rioul, M. Vetterli, Wavelets and signal processing, IEEE Signal Process. Mag. (October 1991).
[25] B.M. Sadler, A. Swami, Analysis of multiscale products of step detection and estimation, IEEE Trans. Inform. Theory 45 (3) (April 1999).
[26] E.P. Simoncelli, W.T. Freeman, E.H. Adelson, D.J. Heeger, Shiftable multiscale transforms, IEEE Trans. Inform. Theory 38 (2) (1992) 587–607.
[27] A. Swami, G.B. Giannakis, Signal detection and classification in multiplicative and additive noise, Proceedings of the IEEE Workshop on Non-linear Signal and Image Processing, June 1995, pp. 20–22.
[28] J.-Y. Tourneret, Detection and estimation of abrupt changes contaminated by multiplicative Gaussian noise, Signal Processing 68 (3) (August 1998) 259–270.
[29] H.L. van Trees, Detection, Estimation, and Modulation Theory, Wiley, New York, 1968.
[30] M. Vetterli, J. Kovacevic, in: A.V. Oppenheim (Ed.), Wavelets and Subband Coding, Prentice-Hall Signal Processing Series, Prentice-Hall, Englewood Cliffs, NJ, 1995.
[31] L.G. Weiss, Wavelets and wideband correlation processing, IEEE Signal Process. Mag. (January 1994) 13–32.
[32] R.K. Young, Wavelet Theory and its Applications, Kluwer, Dordrecht, 1993.